Current Science
CS 4 (6), 846– 852 (2024)
Received 22 **August** 2024 | **Revised** 20 **Sept** 2024 | **Accepted** 25 **Oct**. 2024 | **Online Available** 30 **November** 2024
https://doi.org/10.52845/CS/2024-4-6-8

Current Science

Current Science

OPEN ACCESS

ISSN(O)2795-8639

ORIGINAL ARTICLE

An Inventional De-Embedding Technique for Signal Leakage Up to 110 ghz

Dan He[1], Hao Min[2]

[1]Integrated Circuit Engineering, School of Microelectronics, Fudan University, China 201210

[2]School of Microelectronics, Fudan University, China 201210

***Corresponding Author: Dan He**

Abstract

An inventional de-embedding technique is presented in this letter for signal leakage up to 110GHz. Specifically, it used open and short structures without needing additional de-embedding structures. It equates RF signal pad to ground as Rsub and Csub connected in parallel and then connected in series with Cox compared with traditional open short de-embedding, which equates the RF signal pad to ground as a lumped capacitance and is no longer applicable when the frequency exceeds 10GHz due to the signal leaking from the RF signal pad to the psub ground. The proposed de-embedding technique has been validated on RF parameters of NMOS device up to 110 GHz with physical trend and 34.3% improvement in de-embedding accuracy.

***Index Terms*—de-embedding, millimeter wave, RF modeling**

Introduction

THERE are two major solutions for 5G: Sub-6G and millimeter wave. At present, the vast majority of RF modeling still remains within the frequency range of 10GHz. This is far from enough for millimeter wave design. 110GHz RF modeling is the main modeling solution for 5G applications. The implementation of 110GHz RF modeling requires the stability of the RF testing system, the rationality of the RF testkey design, the accuracy of the de-embedding method, and the accuracy of the modeling method. The above aspects are indispensable. Only by establishing an accurate RF model can make sure the high frequency characteristics of the device be accurately characterized and provide a solid foundation for successful millimeter wave circuit design by circuit designers.

Calibration methods such as SOLT and LRRM are used to move the calibrated reference surface to the tip of the needle, and the parasitic effects from the tip to the DUT need to be removed using a de-embedding method. And calibration techniques can be divided into two categories. The first type can be attributed to the lumped equivalent circuit model de-embedding technique, while the second type can be attributed to the cascaded de-embedding technique.

The first type of de-embedding technology[1]-[7]: These models configure probe pins, metal interconnects, and semiconductor substrates in parallel series. After subtracting parasitic components from the admittance and impedance matrices, unnecessary parasitic components are removed. As the operating frequency enters the range of tens of GHz, metal interconnects become longer electrically. Equivalent circuit methods may not work well as they only consider the resistance and inductance effects of metal interconnects.

The second type of de-embedding technology[8]-[11]: These models the probe pins, interconnects, and DUT as cascaded connections between two ports. Their development is aimed at overcoming the drawbacks of equivalent circuit de-embedding methods. Although the de-embedding method based on cascading at both ends can accurately calculate and eliminate the parasitic effects of pins and interconnects, it ignores the parasitic effects

of source suspended legs.

De-Embedding Principle

RF MOS testkey including dut, open, short de-embedding structure were designed, fabricated and 110GHz S parameter were measured with Keysight PNA and B1500 in Formfactor probe station. Fig.1 shows Layout of DUT and de-embedding structure open, short. 3um by 11um metal1 slot was designed for study signal leakage.

Traditional open short de-embedding method were adopted. It was found that Cgs and Cgd at different Vgs and Vds bias increase with increasing frequency especially over 10GHz, which is unreasonable as shown in Fig.2. After extensive experiments and theoretical analysis, this phenomenon can be attributed to the fact that traditional de-embedding is no longer applicable in frequencies greater than 10GHz.

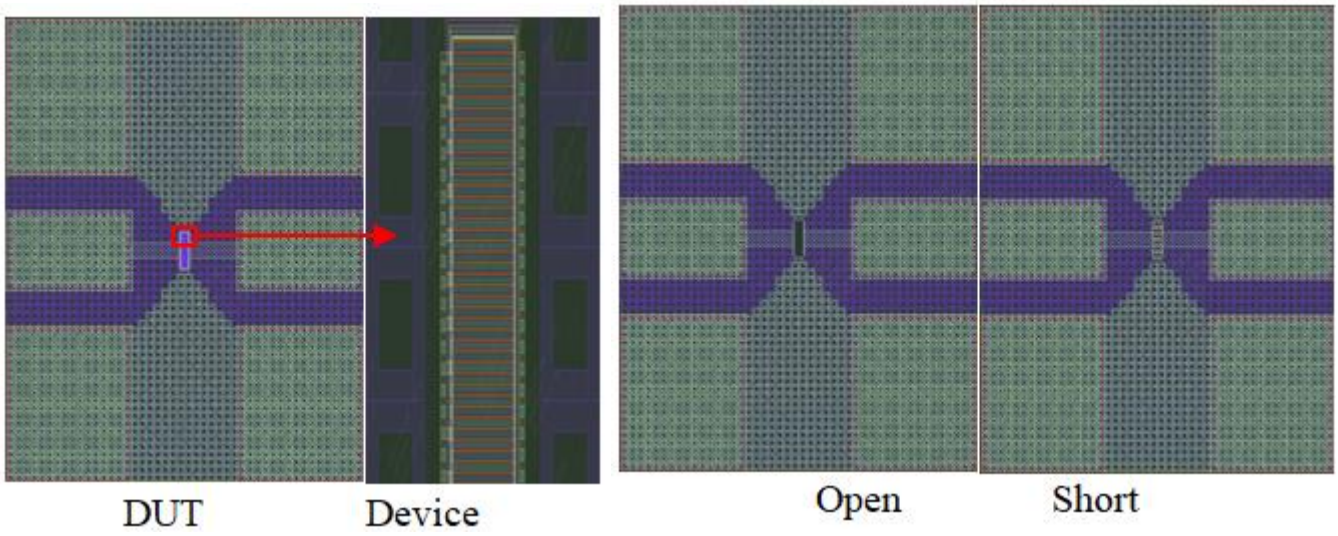

Figure 1 Layout of DUT and de-embedding structure

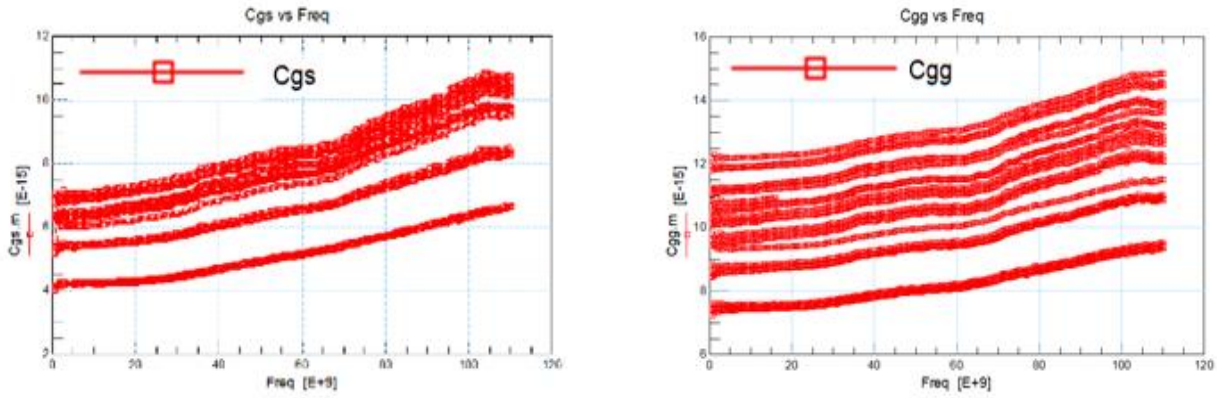

Figure 2 Cgs and Cgg increase with traditional open short de-embedding method

When designing RF GSG pads, metal1 is usually used as the shielding layer below the signal. When the process evolves to an advanced node, the design rules do not allow metal1 to be a whole piece, and there must be a metal slot. So even if metal1 is used as shielding, there is still a portion of the signal leaking from the RF signal pad to the psub ground. Therefore, the traditional open short de-embedding method equates the RF signal pad to ground as a lumped capacitance, which is no longer applicable when the frequency exceeds 10GHz. This paper proposes a new method of de-embedding, which equates RF signal pads to ground as Rsub and Csub are connected in parallel and then connected in series with Cox.

A. Traditional Open Short De-embedding Method

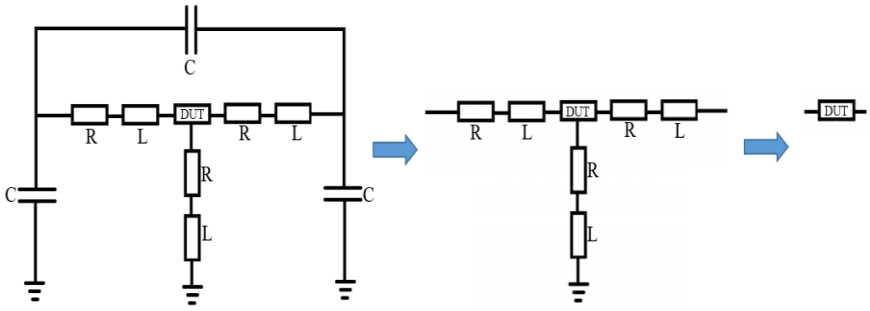

B. Inventional De-embedding Method (0-110GHz)

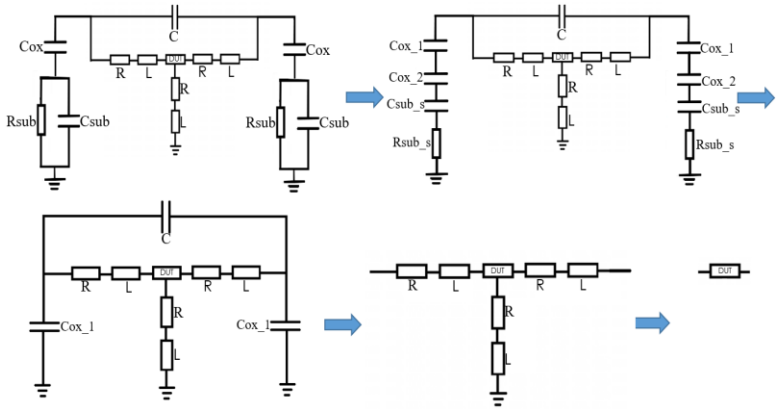

RF MOS is a two port network (Gate is port 1, Drain is port 2, Source and Bulk are grounded). The RF signal pad to ground can be equivalent to the following circuit structure with Y parameters of Y11+Y12.

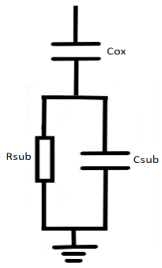

$$Y11 + Y12 = \frac{j\omega Cox(\frac{1}{Rsub} + j\omega Csub)}{j\omega Cox + \frac{1}{Rsub} + j\omega Csub} \quad (1)$$

$$Re(Y11 + Y12) = \frac{RsubCoxCox}{\frac{1}{\omega^2} + Rsub^2(Cox + Rsub)^2} \quad (2)$$

$$Im(Y11 + Y12) = \frac{Cox\frac{1}{\omega}}{\frac{1}{\omega^2} + Rsub^2(Cox + Rsub)^2} \quad (3)$$

$$slope = \frac{Re(Y11 + Y12)}{Im(Y11 + Y12)\omega} = RsubCox \quad (4)$$

$$\frac{\mathrm{Im}(Y11+Y12)}{\omega}=\frac{\mathrm{Cox}}{1+\omega^2\mathrm{Rsub}^2(\mathrm{Cox}+\mathrm{Csub})^2} \quad (5)$$

When Freq=69GHz, the capacitance to ground (imag (Y11+Y12)/(2*pi*Freq)) reaches a turning point, at which point the admittance of Rsub and Csub is equal as shown in Fig.3. From (5), before this frequency, Rsub dominates. After this frequency, Csub dominates. Before 69GHz, the decrease in Im (Y11+Y12)/(2*pi*Freq) with increasing frequency was caused by Rsub. Assuming that the signal pad to ground circuit is equivalent to Cox and Csub in series, then Im (Y11+Y12)/ (2*pi*Freq) is flat with frequency.

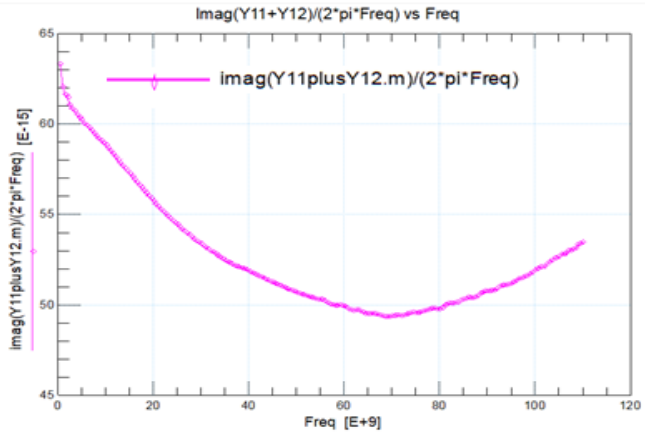

Figure 3 Imag (Y11+Y12)/(2*pi*Frequency) vs Frequency plot

$$\mathrm{Rsub}=\frac{1}{2*\mathrm{pi}*69e9*\mathrm{Csub}} \quad (6)$$

By solving the above equation, analytical solutions for Cox, Rsub, and Csub can be obtained.

$$\mathrm{Cox}=\mathrm{Re}(Y11+Y12)\left[\frac{1}{\omega^2}+\mathrm{slope}^2\left(1+\frac{1}{2*\mathrm{pi}*69e9*\mathrm{slope}}\right)^2\right]\frac{1}{\mathrm{slope}} \quad (7)$$

$$\mathrm{Rsub}=\frac{\mathrm{slope}}{\mathrm{Cox}} \quad (8)$$

$$\mathrm{Csub}=\frac{1}{2*\mathrm{pi}*69e9*\mathrm{Rsub}} \quad (9)$$

The solution results for Cox, Csub, and Rsub are as shown in Fig.4. They vary with frequency.
From (7), Cox increases with frequency and is influenced by Re (Y11+Y12). From (8) and (9), Cox increases with frequency, leading to a decrease in Rsub and an increase in Csub with frequency.

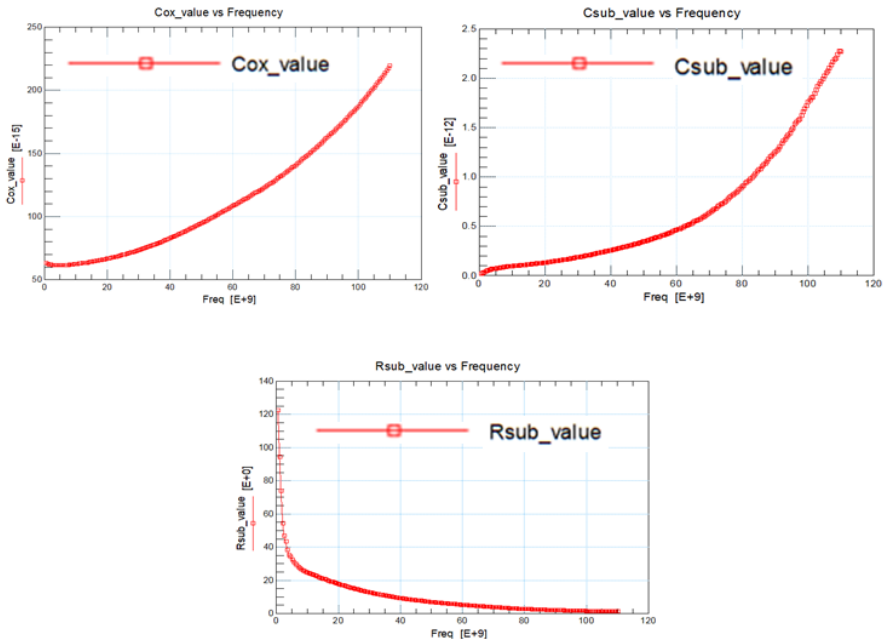

Figure 4 Cox,Csub,Rsub vs Frequency plot

Then bring the analytical solutions of Cox, Csub, and Rsub into (2) and (3), calculate real(Y11+Y12) and imag (Y11+Y12), and compare them with the measured data, and the two coincide as shown in Fig.5.

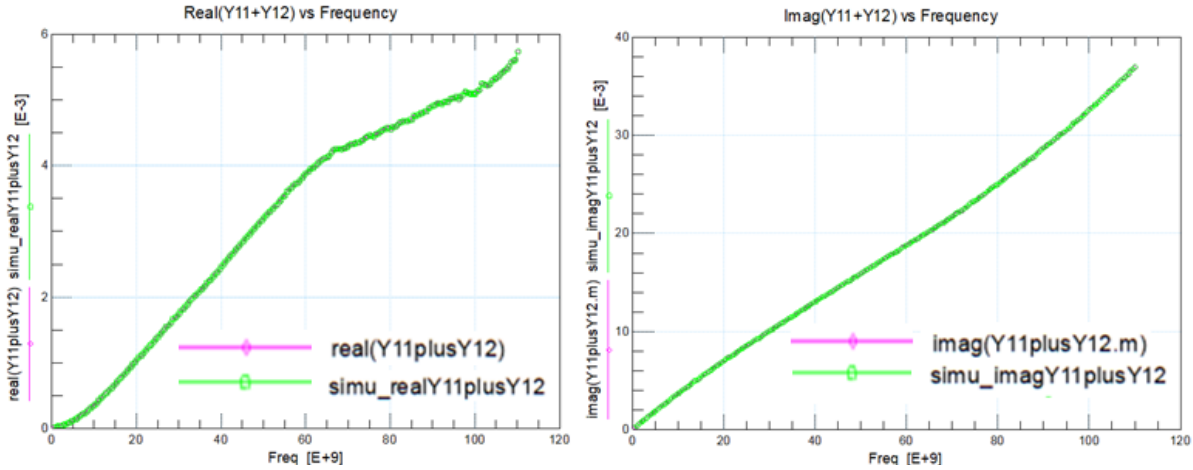

Figure 5 Real(Y11+Y12) and Imag(Y11+Y12) vs Frequency plot

Convert Rsub and Csub in parallel to Rsub_s and Csub_s in series. Split Cox into two parts: Cox_1 and Cox_2. Cox_1 is frequency independent, while Cox_2 is frequency dependent.
Suppose Cox and Rox in series,

$$Y = \frac{1}{Rox + \frac{1}{j\omega Cox}}$$

$$ImY = \frac{\omega Cox}{(Rox(\omega Cox))^2 + 1}$$

(ωCox)2~(e9*e-15)2~e-12<<1, ImY/ω~Cox

Suppose Cox and Rox in parallel,

ImY/ω=Cox.

So the frequency related components of Cox are caused by Rsub and Csub. If metal 1 shielding is done well enough, Cox will not exhibit frequency related components. Cox_1 is retained in the proposed de-embedding method.

III. Validation

RF MOS testkey including dut, open and short de-embedding structure were designed and fabricated in 28HKC process with different width, length and finger number. 110GHz S parameters were measured with Keysight PNA and B1500 in Formfactor probe station. The inventional de-embedding results compared with traditional de-embedding results are shown in Fig.6 and Fig.7.

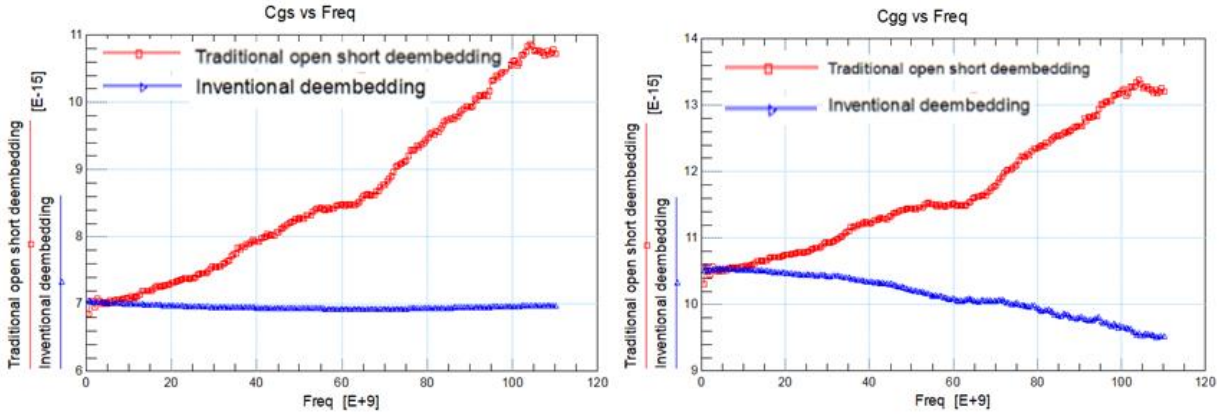

Figure 6 Cgs and Cgg with inventional de-embedding method and traditional open short de-embedding method

The inventional de-embedding technique is physical compared with traditional open short de-embedding method due to the signal leaking from the RF signal pad to the psub ground. The proposed de-embedding technique has been validated on RF parameters of NMOS device for up to 110 GHz. Cgs is 10.6Ff and 6.964Ff at 100GHz with two de-embedding technique, and the difference is 34.3%. So The proposed de-embedding technique has 34.3% improvement in de-embedding accuracy.

Conclusion

An inventional de-embedding technique is presented in this letter for signal leakage up to 110GHz. When the process evolves to an advanced node, the design rules do not allow metal1 to be a whole piece, and there must be a metal slot. So even if metal1 is used as shielding, there is still a portion of the signal leaking from the RF signal pad to the psub ground. The traditional open short de-embedding method equates the RF signal pad to ground as a lumped capacitance, which is no longer applicable when the frequency exceeds 10GHz. This paper proposes a new method of de-embedding, which equates RF signal pads to ground as Rsub and Csub are connected in parallel and then connected in series with Cox. The proposed de-embedding technique has been validated on RF parameters of NMOS device for up to 110 GHz with physical trend and 34.3% improvement in de-embedding accuracy.

References

1. P. J. Van Wijnen, H. R. Claessen, and E. A. Wolsheimer, “A new straightforward calibration and correction procedure for ‘on wafer’ high frequency S-parameter measure-ements (45 MHz–18 GHz),” in Proc. IEEE Bipolar Circuits Technol. Meeting, Sep. 1987, pp. 70–73.
2. M. C. A. M. Koolen, J. A. M. Geelen, and M. P. J. G. Versleijen, “An improved de-embedding technique for on-wafer high-frequency characterization,” in Proc. Bipolar Circuits Technol. Meeting, Minneapolis, MN, USA, Sep. 1991, pp. 188–191.
3. H. Cho and D. E. Burk, “A three-step method for the de-embedding of high-frequency S-parameter measurements,” IEEE Trans. Electron Devices, vol. 38, no. 6, pp. 1371–13 75, Jun. 1991.
4. [4] E. P. Vandamme, D. M. M. Schreurs, and G. van Dinther, “Improved three-step de-embedding method to accurately account for the influence of pad parasitics in silicon on-wafer RF test-structures,” IEEE Trans.

Electron Devices, vol. 48, no. 4, pp. 737–742, Apr. 2001.
5. R. Torres-Torres, R. Murphy-Arteaga, and J. Reynoso-Hernandez, "Analytical model and parameter extraction to account for the pad parasitics in RF-CMOS," IEEE Trans. Electron Devices, vol. 52, no. 7, pp. 1335–1342, Jul. 2005.
6. T. E. Kolding, "A four-step method for de-embedding gigahertz on-wafer CMOS measurements," IEEE Trans. Electron Devices, vol. 47, no. 4, pp. 734–740, Apr. 2000.
7. L. F. Tiemeijer, R. J. Havens, A. B. M. Jansman, and Y. Bouttement, "Comparison of the 'pad-open-short' and 'open-short-load' deembedding techniques for accurate on-wafer RF characterization of high quality passives," IEEE Trans. Microw. Theory Techn., vol. 53, no. 2, pp. 723–729, Feb. 2005.
8. C.-H. Chen and M. J. Deen, "A general noise and S-parameter deembedding procedure for on-wafer high-frequency noise measurements of MOSFETs," IEEE Trans. Microw. Theory Techn., vol. 49, no. 5, pp. 1004–1005, May 2001.
9. M.-H. Cho et al., "A shield-based three-port de-embedding method for microwave on-wafer characterization of deep-submicrometer silicon MOSFETs," IEEE Trans. Microw. Theory Techn., vol. 53, no. 9, pp. 2926–2934, Sep. 2005.
10. Issaoun, Y. Z. Xiong, J. Shi, J. Brinkhoff, and F. Lin, "On the deembedding issue of CMOS multigigahertz measurements," IEEE Trans. Microw. Theory Techn., vol. 55, no. 9, pp. 1813–1823, Sep. 2007.
11. Zhang, Y.-Z. Xiong, L. Wang, S. Hu, and J. L.-W. Li, "On the de-embedding issue of millimeter-wave and sub-millimeter-wave measurement and circuit design," IEEE Trans. Compon., Packag., Manuf. Technol., vol. 2, no. 8, pp. 1361–1369, Aug. 2012.

Dan He received the B.S. and M.S. degree in electrical engineering from Hangzhou Dianzi University, China in 2007, and is currently working toward the Ph.D. degree at Fudan University.
Her research interests mainly focus on RF device design, layout optimization, high-frequency de-embedding and modeling.

Hao Min received the B.S. and M.S. degree in electrical engineering from Fudan University, Shanghai, China in 1985 and 1988 respectively. In 1991 he received the PH.D. degree in material science from Fudan. From 1996 to 1998 he was a visiting scholar in Stanford University, CA. He is now the director of ASIC and System State Key Laboratory. He has published more than ten technical papers in journals and conferences. His research interests include mixed signal VLSI design and digital signal processing.